Influence of the transducer near field in MR elastography wave images

S. Papazoglou[1], J. Rump[1], D. Klatt[1], U. Hamhaber[2], J. Braun[2], I. Sack[1]

[1]Charite, CCM, Institute of Radiology, Berlin, Germany, [2]Charite, CBF, Institute of Medical Informatics, Berlin, Germany

Introduction: Soft biological tissues can be assumed to be incompressible in a first approximation [1], since shear waves lengths are typically of the order of centimetres, while the wave lengths of pressure waves are of the order of meters. Here, it is shown that a longitudinal component at approximately shear wave length can be observed in MRE experiments on gelatine, if a piston source is used which works in compressional mode. It is shown by comparison to simulations that the longitudinal component cannot be attributed solely to the shear field suggesting considerable influence due to the near field. Since the near field shows wave lengths larger than shear wave length at very short distances [2], this could lead to biases in elasticity estimates close to boundaries, where new sources show up as response to incident waves. In particular this could contribute to wrong conclusions about the exact boundaries of an inclusion by MRE.

Theory: In a homogenous, isotropic, linear elastic material the elastic field in full space due to a point source can be written as the sum of three parts (see i.e. [3])

$$\vec{u} = \vec{u}^{(p)} + \vec{u}^{(s)} + \vec{u}^{(c)} \qquad (1)$$

Here the uppercase p stands for the pressure field, s denotes the shear field and c the so-called coupling field. Since the latter significantly contributes only near the source it is also often referred to as the near field. It should be noted at this point that none of the three components of this decomposition is curl-free or divergence-free. This is because the near field comprises terms that are shear and terms that are compressional. The explicit expressions for the Cartesian components of the total field due to a sinusoidal source at the origin acting in x-direction reads

$$u_i^{(p)}(\vec{r},t) = \frac{1}{4\pi\rho c_p^2}\frac{x\cdot x_i}{r^2}\frac{1}{r}\sin\left[2\pi f\left(t - r/c_p\right)\right] \qquad (2)$$

$$u_i^{(s)}(\vec{r},t) = \frac{1}{4\pi\rho c_s^2}\left(\delta_{1i} - \frac{x\cdot x_i}{r^2}\right)\frac{1}{r}\sin\left[2\pi f\left(t - r/c_s\right)\right]$$

$$u_i^{(c)}(\vec{r},t) = \frac{1}{4\pi\rho}\left(\frac{3x\cdot x_i}{r^2} - \delta_{1i}\right)\frac{1}{r^3}\int_{r/c_p}^{r/c_s}\tau\sin\left[2\pi f\left(t-\tau\right)\right]d\tau$$

Here, c_p is the speed of the pressure wave, c_s is the shear wave speed, ρ is the material density and f is the excitation frequency. The index i takes value *1,2,3* corresponding to Cartesian *x,y,z*. According to Huygen's principle the field of an extended source is obtained by summing over the whole surface of the source

$$U_i(\vec{r},t) = a\iint u_i(\vec{r}-\vec{r}',t)\,dS(\vec{r}') \qquad (3)$$

where a is the strength of the source. Eqs. 1, 2 and 3 were used for the numerical simulation of elastic fields in full space.

Methods: MRE experiments were performed on a 1.5 T scanner (Siemens Sonata, Germany). A modified EPI sequence incorporating sinusoidal motion encoding gradients along the slice-select direction was used for image acquisition. A transversal image slice was used defining our physical coordinate system with x parallel to the phase-encode direction and z perpendicular to the image slice. Vibrations were introduced into a gelatine phantom by a piston attached to the surface at $z = 0$. The piston worked in compressional mode i.e. displacement was perpendicular to the surface of the phantom in x-direction. Piston diameter was 2.4 cm and excitation frequency was 299.4 Hz. 41 wave images were acquired encompassing a whole cycle of wave propagation. Both x- and z-components of the shear wave field were in consecutive experiments. Simulations were performed using eq.3 and experimental parameters as excitation frequency, initial wave amplitude and piston size.

Results: The experimentally measured wave components were reproduced by simulations using 4.6 m/s for the shear wave speed and 1500 m/s for the compressional wave speed. In fig. 1a a longitudinal component can clearly be seen on axis. The wave length of this component is approximately the same as for the shear wave which is perspicuous by comparison to fig. 1b. The corresponding simulations (figs. 1c and 1d) show essentially the same patterns. Differences are due to surface effects as Rayleigh waves and head waves [4] as well as viscous damping, not included in the simulations.

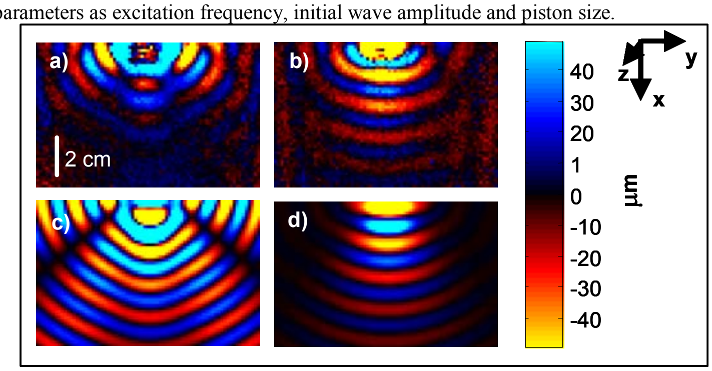

Fig. 1) Experimental data for a) displacement in excitation direction showing a longitudinally polarized wave on the x-axis, **b)** displacement perpendicular to the excitation direction showing primarily the shear field; **c)** and **d)** show corresponding simulated data.

Discussion: The longitudinal wave observed in fig. 1a is partly due to shear waves propagating at an angle with respect to the x-axis and thereby having a displacement component parallel to the encoding direction. The contribution due to the near field can be seen from fig. 3, where the shear term and the near field term are shown separately. The sum of the two wave images results in fig. 2c. By comparing the amplitudes in fig. 3a and b it is readily seen, that the near field term is not negligible up to several shear wave lengths away from the source. In a more realistic situation viscosity will damp the waves away rather quickly as seen in fig. 1a. Nevertheless, close to the source the near field term contributes significantly resulting in the dilated wave shape around the x-axis as it was found in our experiments.

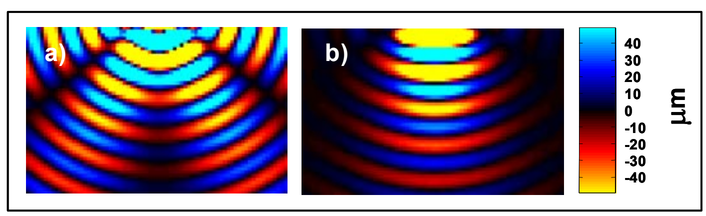

Fig. 2) Separate terms according to eq. 2; **a)** shows the shear field term and **b)** the near field. Note, both field amplitudes are in the same order!

Conclusion: It was shown, that a longitudinal component at shear wave length can be observed in MRE experiments on a gelatine phantom. It was demonstrated that this component is partly due to shear vibrations and partly due to the near field wave. This was underlined by comparison of the amplitudes of the separate shear and near field terms as available from numerical simulation.

References:

[1] Sinkus R., Magn. Res. Med. **53,** 372-387 (2005)

[2] Sandrin L. et al, J. Acoust. Soc. Am. **115**(1) , 73-83 (2004)

[3] Aki K., Richards P. G., Quantitative Seismology, University Science Books (2002)

[4] Benech N., Negreira C. A., J. Acoust. Soc. Am. **117**(6), 3424-3431 (2005)